

https://dspace.org/

Tumor Necrosis Factor- Mediates Inflammation-induced Early-Stage Left Ventricular Systolic Dysfunction

Manilall, Ashmeetha; Mokotedi, Lebogang; Gunter, Sulè; Le Roux, Regina; Fourie, Serena ...

2023
Lippincott
https://hdl.handle.net/10539/50224
Manilall, A., Mokotedi, L., Gunter, S., Le Roux, R., Fourie, S., Flanagan, C. A., & Millen, A. M. E. (2023). Tumor Necrosis Factor- Mediates Inflammation-induced Early-Stage Left Ventricular Systolic Dysfunction. Journal of Cardiovascular Pharmacology, 81(6), 411–422. https://doi.org/10.1097/FJC.0000000000001428

Downloaded from a DSpace repository. https://dspace.org/

Tumor Necrosis Factor-α Mediates Inflammation-induced Early-Stage Left Ventricular Systolic Dysfunction

Ashmeetha Manilall, PhD, Lebogang Mokotedi, PhD, Sulè Gunter, PhD, Regina Le Roux, MSc, Serena Fourie, MSc, Colleen A. Flanagan, PhD, and Aletta M. E. Millen, PhD

Abstract: Elevated systemic inflammation contributes to pathogenesis of heart failure with preserved ejection fraction (HFpEF), but molecular mechanisms are poorly understood. Although left ventricular (LV) diastolic dysfunction is the main cause of HFpEF, subclinical systolic dysfunction also contributes. We have previously shown that rats with collagen-induced arthritis (CIA) have systemic inflammation, LV diastolic dysfunction, and that increased circulating TNF-α contributes to inflammation-induced HFpEF pathogenesis, but does not mediate LV diastolic dysfunction in CIA rats. Contribution of systemic inflammation to dysfunction of the active process of LV diastolic and systolic function are unknown. In the present study, we used the CIA rat model to investigate the effects of systemic inflammation and TNF-α blockade on systolic function, and mRNA expression of genes involved in active diastolic relaxation and of myosin heavy chain (MyHC) isoforms. Collagen inoculation and TNF-α blockade did not affect LV mRNA expression of genes that mediate active LV diastolic function. Collagen-induced inflammation impaired LV global longitudinal strain ($P = 0.03$) and velocity ($P = 0.04$). This impairment of systolic function was prevented by TNF-α blockade. Collagen inoculation decreased mRNA expression of α-MyHC (*Myh6,* $P = 0.03$) and increased expression of β-MyHC (*Myh7,* $P = 0.0002$), a marker, which is upregulated in failing hearts. TNF-α blockade prevented this MyHC isoform-switch. These results show that increased circulating TNF-α changes the relative expression of MyHC isoforms, favoring β-MyHC, which may underlie changes in contractile function that impair systolic function. Our results indicate that TNF-α initiates early-stage LV systolic, rather than LV diastolic dysfunction.

Received for publication September 24, 2022; accepted March 28, 2023.

From the School of Physiology, Faculty of Health Sciences, University of the Witwatersrand, Johannesburg, South Africa.

The authors report no conflict of interest.

This study was supported by the National Research Foundation (Thuthuka programme, Grant number TTK180419322656) and the Faculty of Health Sciences Research Committee at the University of the Witwatersrand.

A. Manilall: investigation, validation, writing—original draft preparation, visualization; **L. Mokotedi:** methodology, writing—review and editing; **S. Gunter:** methodology, writing—review and editing; **R. Le Roux:** investigation; **Serena Fourie:** investigation; **C. A Flanagan:** validation, writing—review and editing; **A. M. E. Millen:** Conceptualization, validation, formal analysis, project administration, funding acquisition, supervision.

Correspondence: Ashmeetha Manilall, PhD, Molecular Physiology Laboratory, School of Physiology, Faculty of Health Sciences, University of the Witwatersrand Medical School, 7 York Road, Parktown, 2193, Johannesburg, South Africa (e-mail: ashmeetha.manilall@wits.ac.za).

Copyright © 2023 Wolters Kluwer Health, Inc. All rights reserved.

Key Words: tumor necrosis factor-alpha inhibitor, myosin heavy chain, speckle-tracking echocardiography, LV systolic function

(*J Cardiovasc Pharmacol*™ 2023;81:411–422)

INTRODUCTION

It has been proposed that elevated systemic inflammation that results from autoimmune and metabolic disorders causes heart failure with a preserved ejection fraction (HFpEF).[1–3] HFpEF accounts for up to 50% of heart failure cases and therapeutic management is difficult.[4–6] It has been suggested that better understanding of the mechanisms of HFpEF pathogenesis may contribute to enhanced therapeutic options.[5] Left ventricular (LV) diastolic dysfunction is believed to be the main cause of HFpEF and patients with LV diastolic dysfunction frequently progress to overt HFpEF.[7,8] However, many patients with HFpEF also exhibit subclinical myocardial systolic dysfunction.[9–13]

Rats with collagen-induced arthritis (CIA) provide a useful model of chronic systemic inflammation that does not have the confounding metabolic effects inherent in many other models. We have previously shown that collagen inoculation of rats increases circulating inflammatory cytokines and causes LV diastolic dysfunction.[14,15] We have also shown that rats with CIA exhibit partial disruption of systolic function.[15] Although we have not demonstrated overt heart failure, these data suggest that rats with CIA are in the early stages of pathogenesis toward HFpEF and could provide a model for studying the earliest mechanisms of inflammation-induced HFpEF.

LV diastolic function depends on active and passive processes.[5] Adverse extracellular matrix remodeling[16] and hypophosphorylation of the giant spring protein, titin,[17] contribute to passive myocardial stiffness, which affects the ability of the heart to relax during diastole. We have previously shown that rats with CIA have increased profibrotic gene expression LV fibrosis[18] and disrupted expression of genes that regulate titin phosphorylation,[19] showing that systemic inflammation disrupts the passive processes of diastolic function. However, it is not known whether the active process of diastole is affected by the systemic inflammation in rats with CIA.

In the active process of diastole, mitochondria generate ATP that is exported to the cytoplasm where it is used for detachment of actin-myosin cross bridges and for sequestration of Ca^{2+} from the cytoplasm into the sarcoplasmic reticulum (SR) via sarcoplasmic reticulum calcium ATPase (SERCA2a).[20] Decreased SERCA2a function because of

Copyright © 2023 Wolters Kluwer Health, Inc. Unauthorized reproduction of this article is prohibited.

decreased mitochondrial production of ATP or reduced SERCA2a expression, impairs the ability of the SR to sequester Ca^{2+}. The resulting accumulation of Ca^{2+} in the cytoplasm increases diastolic tension and impairs cardiomyocyte relaxation.[5,20–22] Inflammatory cytokines have been reported to impair processes involved in intracellular Ca^{2+} transport, including the expression and activity of SERCA2a in cultured cells.[23,24]

Tumor necrosis factor-α (TNF-α) has been proposed to be the major circulating cytokine that mediates pathogenesis of HFpEF that is induced by chronic systemic inflammation.[25,26] However, clinical trials of various therapeutics that decrease or block circulating TNF-α have shown variable effects on cardiac function[14,27,28] and we have shown that blockade of circulating TNF-α does not prevent development of LV diastolic dysfunction in the CIA rat model.[14] However, we have shown that TNF-α, at least partially, mediates inflammation-induced LV remodeling and increases profibrotic gene expression[18] and also disrupts expression of some of the genes that regulate titin phosphorylation.[19]

Besides diastolic abnormalities, subclinical myocardial systolic dysfunction has been reported in patients with HFpEF.[9–13] Subclinical systolic dysfunction has also been reported in patients with chronic systemic inflammatory conditions[29–33] and associated with increased levels of circulating inflammatory markers.[30,31] We have recently shown associations between inflammatory markers and impaired myocardial systolic function as measured by speckle tracking echocardiography (STE) in the CIA rat model.[15] However, the cellular processes underlying inflammation-induced impairment in myocardial deformation and motion[7] and the contribution of increased circulating TNF-α are currently not known.

Although increased systemic inflammation is known to contribute to the pathogenesis of HFpEF,[34,35] the molecular mechanisms of LV diastolic dysfunction and the role of increased circulating TNF-α are poorly understood. We have used the CIA rat model, without and with blockade of circulating TNF-α, to assess the effects of systemic inflammation and TNF-α on the LV tissue mRNA expression of genes that code for proteins that play a role in Ca^{2+} sequestration, mitochondrial function, and apoptosis in LV tissue. We have also assessed the direct effects of TNF-α on a human cardiomyocyte-derived cell line. Because TNF-α does not mediate LV diastolic dysfunction, we have used the CIA rat model, without and with blockade of circulating TNF-α, to assess the contribution of TNF-α to development of early-stage systolic dysfunction and the effects of inflammation and TNF-α on the expression of isoforms of the myosin heavy chain (MyHC) contractile protein.

METHODS

Animal Treatment and Sample Collection

All experimental procedures were approved by the Animal Ethics Screening Committee of the University of the Witwatersrand (AESC approval: 2017/03/21C) and conducted in accordance with the Guide for the Care and Use of Laboratory Animals. 3-month-old Sprague-Dawley rats were randomly assigned to 3 groups. Systemic inflammation was induced in 2 groups using a modified Chondrex collagen inoculation protocol.[11] Briefly, rats were injected subcutaneously, at the base of the tail, with Bovine type II collagen (2 mg/mL in 0.05 M acetic acid) emulsified in incomplete Freund's adjuvant (1:1 volume, 0.2 mL). Booster injections (0.1 mL) were administered 7 and 21 days after the first immunization. The 2 groups inoculated with collagen consisted of the CIA group (n = 26) that received no further treatment and the TNF-α blocker (CIA+anti-TNF-α) group (n = 16) that were treated with the TNF-α binder, etanercept (Enbrel, 10 mg/kg-1, Amgen Inc., Thousand Oaks, CA) every 3 days for 6 weeks after development of arthritis. The lower number of rats in the CIA+anti-TNF-α group was because of the expense of the etanercept. Rats in the control (con) group (n = 31) received a subcutaneous injection of saline (0.2 mL). Because incomplete Freund's adjuvant alone is known to induce arthritis and to stimulate inflammation, including expression of TNF-α, in rodents,[36] saline was used to ensure that control rats had no induced inflammation to allow assessment of the effects of increased systemic inflammation on LV function and gene expression in CIA rats. Tail cuff blood pressure was measured every 2 weeks at midday using non-invasive blood pressure amplifiers (Biopac Systems, Santa Barbara, CA, United States) as previously described.[14] Arthritis scores and paw thickness in rat hind paws were assessed using a 0–4 grading scale[37] and a digital calliper, respectively, as previously described.[14] The rats used in the current study are part of a larger ongoing study of the effects of collagen-induced systemic inflammation.[14] In accordance with ethics committee recommendations to minimize numbers of animals used, echocardiography data for a subset (n = 63) of the rats used in the current study have been previously reported. For this study 68 rats (con, 28; CIA, 25: CIA+anti-TNF-α, 15) yielded measurable STE and gene expression (see data analysis).

Echocardiography

Rats were anesthetized by intramuscular injection of ketamine (100 $mg.kg^{-1}$) and xylazine (5 $mg.kg^{-1}$) and echocardiography was performed using an ultrasound (Acuson SC 2000, Siemens Medical Solutions, United States, Inc.) to determine diastolic function and systolic pump function as previously described.[14,15] LV diastolic function was measured using pulsed wave Doppler and Tissue Doppler Imaging. Mitral inflow velocity was measured in the apical 4 chamber view during early (E) and late diastole (A), with the cursor placed at the mitral valve leaflet tips. Tissue Doppler Imaging was used to measure tissue lengthening at the mitral annulus of the lateral wall during early (e') and late (a') periods of diastole. As mitral inflow velocity (E) is dependent on loading conditions and heart rate, whereas e' is relatively preload-independent, the E/e' was calculated as an index of LV filling pressures.[38] Systolic function was determined by calculating the ejection fraction using the Teicholz methods and calculating fractional shortening. In addition, tissue shortening during systole was measured at the lateral annulus using TDI. As more sensitive measures of early-stage LV systolic dysfunction, STE was used to determine

Copyright © 2023 Wolters Kluwer Health, Inc. All rights reserved.

Copyright © 2023 Wolters Kluwer Health, Inc. Unauthorized reproduction of this article is prohibited.

myocardial deformation (LV peak systolic strain and strain rate) and myocardial motion (LV velocity and displacement) in the apical 4 chamber view. B-mode video loops were captured and selected for analysis based on the video quality and well-defined endo- and epicardial borders. To minimize beat-to-beat variability, 5 consecutive cardiac cycles were used for all measures. Automatic border detection software was used to trace the endocardial and epicardial borders, which were manually adjusted to ensure optimal tracking in a frame-by-frame manner. Strain, strain rate, velocity, and displacement were calculated in the longitudinal plane in 6 anatomical regions. Global longitudinal strain, strain rate, displacement, and velocity were calculated as the average of the 6 anatomical segments over 3 consecutive cardiac cycles.

After echocardiography, rats were terminated by thoracotomy. A blood sample was collected, the heart was removed and LV tissue was stored (−80°C) in RNAlater (Ambion, Sigma Aldrich, Germany).

Circulating Inflammatory Markers

Serum concentrations of TNF-α and IL-6 were measured in duplicate by sandwich enzyme-linked immunosorbent assay (ELISA, Elabscience Biotechnology, United States).

Cell Culture and TNF-α Treatment

An immortalized human ventricular cardiomyocyte-derived cell line of unspecified sex, AC16 (Catalogue number 9Q019D; Sigma Aldrich, St. Louis, MO), was used to assess whether changes in gene expression observed in LV tissues reflect direct effects of TNF-α on cardiomyocytes in LV tissues. The AC16 cell line is a fusion of 2 different cell types, 1 of which was a human cardiomyocyte and the other an immortalized human fibroblast. The cardiomyocyte-derived cells provide a model for cardiomyocyte gene expression based on reports that these cells express most of the genes expressed in human cardiomyocytes,[39] although it has recently been shown that the expression is lower than in cardiac tissue.[40] AC16 cells were maintained in HyClone Dulbecco's Modified Eagle Medium (DMEM) + Ham's F-12 medium (GE Healthcare, Chicago, IL), supplemented with 10% foetal bovine serum (Gibco; Thermo Fisher Scientific, Life Technologies, Carlsbad, United States) at 37°C with 5% CO_2. The cells were seeded into 12-well plates using serum-free DMEM + Ham's F-12 medium supplemented with 5% penicillin-streptomycin and allowed to reach ~85% confluence. Cells were then incubated with or without TNF-α (10 ng/mL; Sigma Aldrich, St. Louis, MO) for 5 minutes, 8 hours, or 24 hours with 4 wells per treatment and each experiment was performed 3 times.

Extraction of mRNA and Preparation of cDNA

Rat LV samples were homogenized by sonication and cultured cells were lysed before total RNA extraction using an illustra Mini Spin RNA extraction kit (GE Healthcare, Buckinghamshire, United Kingdom), according to the manufacturer's instructions. The resulting RNA (2 μL) was used to reverse-transcribe messenger RNA to produce cDNA using SuperScript IV VILO cDNA synthesis master mix (18 μL, Thermo Fisher Scientific, Life Technologies, Carlsbad, CA).

Comparative Gene Expression RT-PCR

Comparative gene expression RT-PCR was performed using a StepOne Plus thermocycler (Thermo Fisher Scientific, Life Technologies, Carlsbad, United States) with cDNA (~2 μg), predesigned TaqMan probe mixes for the selected reference gene (0.25 μL), predesigned TaqMan probe mixes for each gene of interest (0.5 μL, TaqMan gene expression assay) and TaqMan advanced PCR master mix (5 μL) in a final volume of 10 μL. Cycling conditions consisted of an initial hold at 50°C for 2 minutes, a hot start hold at 95°C for 10 minutes, followed by 40 cycles at 95°C for 15 seconds and 60°C for 1 minute. The fold-change in relative expression was then calculated as $2^{-\Delta\Delta Ct}$, using the delta-delta Ct method.[41] A RefFinder[42] analysis was performed to select optimal reference genes for RT-PCR from a panel. Hypoxanthine guanine phosphoribosyl-transferase 1 (*Hprt1*) was identified as the most suitable reference gene for the animal model and glyceraldehyde 3-phosphate dehydrogenase (*GAPDH*) was identified as the most suitable reference gene for the cultured cells.

Comparative gene expression of the following genes was assessed in LV tissues using TaqMan probes: *Myh6*, which codes for α-MyHC (Rn00568304_m1); *Myh7*, which codes for β-MyHC (Rn00568328_m1); *SOD2,* which codes for superoxide dismutase 2 (Rn00690588_g1); *SERCA2a*, which codes for SERCA protein (Rn00568762_m1); *S100A1*, which codes for S100A1 protein (Rn01458753_m1); *BAX*, which codes for Bcl-2-associated X-protein (Rn01480161_g1) and *Bcl-2*, which codes for B-cell lymphoma 2 protein (ID: Rn99999125_m1) in duplex reactions with *Hprt1* (Rn01527838_g1, 0.25 μL) in duplicated plates.

The following genes were assessed in AC16 cells using TaqMan probes: *TNF-α* (Hs00174128_m1), *IL-6* (Hs00174131_m1), *SERCA2a* (Hs00544877_m1), *SOD2* (Hs00167309_m1), *Bcl-2* (Hs04986394_s1), and *BAX* (Hs00180269_m1) in duplex reactions with *GAPDH* (Hs99999905_m1, 0.25 μL) in duplicated plates.

Data Analysis

Statistical analyses were performed using SAS software, version 9.4 (SAS Institute Inc., United States). Rats for which 70% or more of the target genes measured for the current study yielded gene expression levels outside the detection limits of the gene expression assays (n = 4) were excluded from the analyses. Data are expressed as mean ± standard error of the mean (SEM). Differences among the groups of rats were determined by two-way analysis of variance (ANOVA) with group and sex as the main effects followed by Tukey post-hoc tests. Because there were no differences in the molecular markers between male and female rats, results were combined. In the AC16 cells, differences between the cells not exposed to TNF-α (control) and those exposed to TNF-α (+TNF-α) were determined by two-way ANOVA with group and time as the main effects,

Copyright © 2023 Wolters Kluwer Health, Inc. All rights reserved.

Copyright © 2023 Wolters Kluwer Health, Inc. Unauthorized reproduction of this article is prohibited.

followed by Tukey *post-hoc* tests. Results were considered statistically significant if $P \leq 0.05$.

RESULTS

Animal Characteristics and Echocardiography Measures of LV Diastolic Function

We have previously reported animal characteristics of CIA and CIA+anti-TNF-α rats.[14] Characteristics of the partially overlapping animals used in the current study are summarized in Table 1. Briefly, LV diastolic function, as indexed by a decreased e' and increased LV filling pressures (E/e') (Table 1), was significantly impaired in the CIA rats, compared with control. The CIA+anti-TNF-α rats also exhibited significant diastolic dysfunction, as indexed by decreased e' and increased LV filling pressures (E/e') (Table 1), compared with control, indicating that blockade of TNF-α did not offset the inflammation-induced LV diastolic dysfunction. Serum TNF-α concentrations were higher in the CIA and CIA+anti-TNF-α rats compared with control group (Table 1). However, the serum CRP concentration in the CIA+anti-TNF-α rats was lower than in the CIA rats (Table 1), confirming that etanercept effectively blockaded the circulating TNF-α in the CIA+anti-TNF-α rats.

Inflammatory Cytokine mRNA Expression in LV Tissue and AC16 Cells

Compared with controls (0.79 ± 0.16), the LV relative mRNA expression of *IL-6* was increased in the CIA rats (1.65 ± 0.13, $P = 0.0004$). However, *IL-6* expression was not increased in the CIA+anti-TNF-α rats (1.15 ± 0.23, $P = 0.40$, Fig. 1A), confirming the anti-inflammatory effects of etanercept. The decreased *IL-6* expression in the CIA+anti-TNF-α rats suggests that increased circulating TNF-α mediates the inflammation-induced increase in IL-6 expression in the CIA group. AC16 cells were incubated with TNF-α, to assess whether TNF-α acts directly on these cardiomyocyte-derived cells to stimulate expression of inflammatory cytokines. The AC16 cells showed increased relative mRNA expression of *IL-6* after exposure to TNF-α for 8 h (27.99 ± 0.59) and 24 h (30.13 ± 4.51), compared with the cells not exposed to TNF-α (8 h: 1.72 ± 0.33, 24 h: 1.01 ± 0.01, both $P < 0.0001$, Fig. 1C).

There were no differences in rat LV tissue relative mRNA expression of *TNF-α* among any of the groups (all $P > 0.05$, Fig. 1B). However, in the AC16 cells, the relative mRNA expression of *TNF-α* was increased in the cells exposed to TNF-α for 8 h (20.05 ± 2.70) and 24 h (16.47 ± 1.37), compared with the control cells (8 h: 1.21 ± 0.17, 24 h: 1.35 ± 0.59, both $P < 0.0001$, Fig. 1d).

Expression of Genes that Regulate Diastolic Calcium Sequestration

The LV tissue relative mRNA expression of *SERCA2a*, which codes for the transporter responsible for Ca^{2+} reuptake into the SR during diastole, was similar in the LV tissues of all the rat groups ($P > 0.05$, Fig. 2A). The relative mRNA expression of *S100A1*, which codes for the Ca^{2+}-binding protein S100A1 that is considered a regulator of SR function, was not different in any of the groups ($P > 0.05$, Fig. 2B). Consistent with the LV tissue results, exposure of the AC16 cells to TNF-α did not affect expression of *SERCA2a* at any time point, compared with the untreated cells (Fig. 2C).

Effect of Collagen Inoculation and anti-TNF-α Treatment on Expression of Genes Involved in Apoptosis

The relative LV tissue mRNA expression of the pro-apoptotic gene; *BAX* (Fig. 3A), and the anti-apoptotic gene; *Bcl-2* (Fig. 3C) were not different in any of the rat groups (all $P > 0.05$). Consistent with these findings, the ratio of *BAX* to *Bcl-2* was also not different in any of the rat groups ($P > 0.05$, Fig. 3E). In the AC16 cells, TNF-α caused a small decrease in relative mRNA expression of *BAX* at 24 h (0.82

TABLE 1. Body Mass, Blood Pressure, Echocardiography Measures, and Circulating Inflammatory Markers in Control, CIA, and CIA+anti-TNF-α Groups

	Control	CIA	CIA+Anti-TNF-α
n (% female)	25 (48)	28 (55)	15 (53)
Body mass (g)	474.2 ± 27.3	421.4 ± 25.7	404.8 ± 35.7
Systolic blood pressure (mm Hg)	129 ± 2	130 ± 2	132 ± 2
Diastolic blood pressure (mm Hg)	87 ± 1	88 ± 1	85 ± 2
Echocardiography			
Lateral wall e' (cm/s)	4.5 ± 0.1	3.6 ± 0.1***	3.5 ± 0.1***
E/e'	25.0 ± 1.2	31.4 ± 1.1**	33.4 ± 1.6**
Lateral wall s' (cm/s)	4.9 ± 0.1	4.5 ± 0.1	4.9 ± 0.2
Circulating inflammatory cytokine concentrations			
TNF-α (pg/mL)	93.9 ± 7.1	155.8 ± 3.9*	145.6 ± 2.9*
IL-6 (pg/mL)	16.4 ± 2.1	29.9 ± 2.0*	27.8 ± 2.6*
CRP (ng/mL)	0.1 ± 0.04	0.6 ± 0.04*	0.4 ± 0.05**

Data are means ± SEM. CIA, collagen-induced arthritis; CIA+anti-TNF-α, collagen-inoculated and treated with TNF-α blocker, etanercept.
* $P < 0.05$ versus control; ** $P < 0.01$ versus control, *** $P < 0.001$ versus control.
$P < 0.05$ versus CIA.

Copyright © 2023 Wolters Kluwer Health, Inc. All rights reserved.

Copyright © 2023 Wolters Kluwer Health, Inc. Unauthorized reproduction of this article is prohibited.

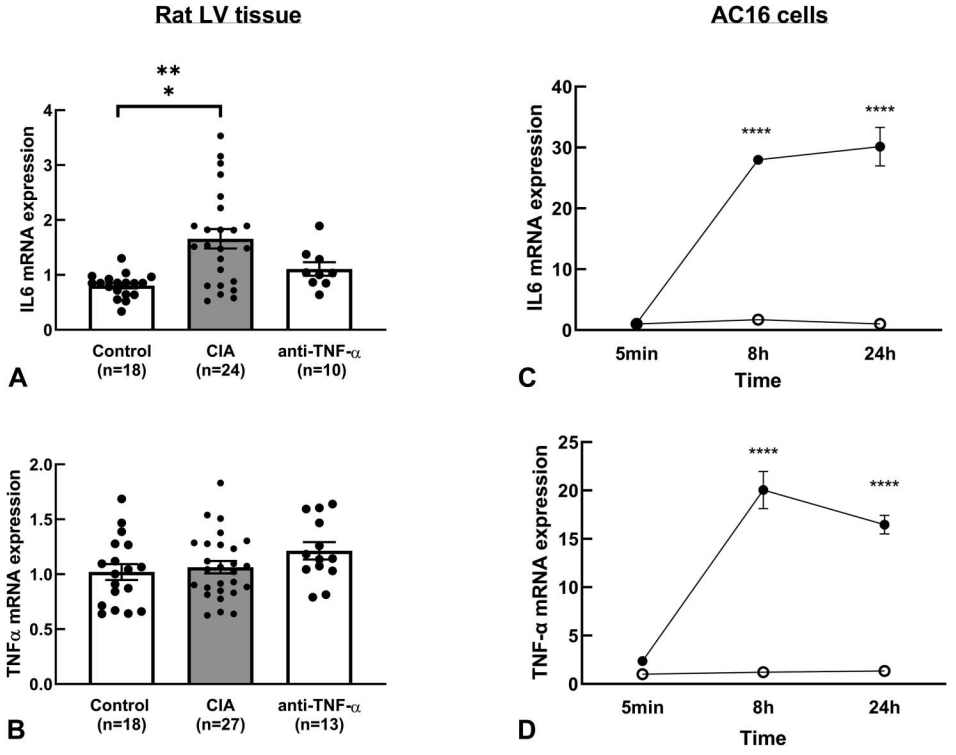


FIGURE 1. Expression of inflammatory cytokine genes in LV tissue and cardiomyocyte (AC16) cells. Rats were inoculated with collagen (CIA) and subsequently treated with a TNF-α blocker (CIA+anti-TNF-α) before measurement of relative mRNA expression of IL-6 (A) and TNF-α (B) in left ventricular tissue (left panel). AC16 cardiomyocytes were incubated without (open symbols) or with TNF-α (filled symbols, 10 ng/mL) before determination of relative mRNA expression of IL-6 (C) and TNF-α (D) (right panel). Results are presented in arbitrary units normalized for the expression of the endogenous reference gene, Hprt1 for LV tissues and GAPDH for AC16 cells, using the ΔΔCt method. Data are means ± SEM. For the AC16 cells, each data point represents the mean ± SEM for 3 independent experiments performed in quadruplicate. ***$P < 0.001$ versus control, ****$P < 0.0001$ versus control.

± 0.07) compared with control cells (1.00 ± 0.05, $P = 0.046$), but had no significant effect at 8 h (Fig. 3B). The relative mRNA expression of *Bcl-2* was decreased in TNF-α-stimulated cells at 8 h (0.72 ± 0.03) compared with control cells (1.00 ± 0.02, $P = 0.04$), and at 24 h (+TNF-α: 0.66 ± 0.10, control: 1.02 ± 0.12, $P = 0.009$, Fig. 3D). The ratio of the relative mRNA expression of *BAX/Bcl-2* was similar in TNF-α-stimulated cells (1.20 ± 0.08) and control cells (1.00 ± 0.01, $P = 0.22$) at 8 h, but was increased in the TNF-α-stimulated cells at 24 h (1.29 ± 0.12) compared with control cells at 24 h (1.01 ± 0.07, $P = 0.046$, Fig. 3F), suggesting a slightly pro-apoptotic state in the AC16 cells exposed to TNF-α.

Effect of Collagen Inoculation and anti-TNF-α Treatment on Expression of a Gene Involved in Mitochondrial Function

The LV, relative mRNA expression of *SOD2*, which is upregulated in mitochondrial oxidative stress, was not different in LV tissue of any of the rat groups ($P > 0.05$, Fig. 4A). In the AC16 cells, *SOD2* mRNA expression was significantly increased in the TNF-α-stimulated cells compared with the cells exposed to control conditions at 8 h (control: 1.01 ± 0.08, +TNF-α: 8.27 ± 0.19, $P < 0.0001$) and 24 h (control: 1.01 ± 0.02, +TNF-α: 9.11 ± 0.41, $P < 0.0001$, Fig. 4B).

Effect of Collagen Inoculation and Anti-TNF-α Treatment on Markers of LV Systolic Function

LV ejection fraction (Fig. 5A), a measure of LV systolic pump function, and midwall fractional shortening (Fig. 5B), a measure of myocardial systolic function, were not different among the rat groups (all $P > 0.05$). The global longitudinal strain, a measure of LV deformation, was impaired in the CIA rats (−16.7 ± 0.76) compared with the control rats (−19.6 ± 0.85, $P = 0.03$, Fig. 5C). The global longitudinal velocity, a measure of LV motion, was impaired in the CIA rats (0.49 ± 0.03) compared with the control rats (0.59 ± 0.03, $P = 0.04$, Fig. 5E). In contrast, the global longitudinal strain and global longitudinal velocity were not different in the CIA+anti-TNF-α group compared with the control group ($P > 0.05$), suggesting that increased circulating TNF-α likely mediates the inflammation-induced LV systolic impairments in the CIA group. The global longitudinal strain ($P = 0.10$) and global longitudinal velocity ($P = 0.79$) were not different between the CIA+anti-TNF-α and CIA groups, indicating incomplete blockade of the inflammation-induced increase in circulating TNF-α or additional TNF-α-independent effects. There were no differences in global longitudinal strain rate (Fig. 5D) or global longitudinal displacement ($P > 0.05$, Fig. 5F) among the groups.

Effect of Collagen Inoculation and Anti-TNF-α Treatment on Expression of Genes Involved in Cardiac Contractility

The relative mRNA expression of *Myh6*, which codes for the α-MyHC isoform, was decreased in CIA rats (0.89 ± 0.04) compared with controls (1.03 ± 0.04, $P = 0.03$). The relative mRNA expression of *Myh6* was significantly higher in the CIA+anti-TNF-α rats (1.11 ± 0.05; $P = 0.004$, Fig. 6A) than in the CIA rats. The relative mRNA expression of *Myh7*,

Copyright © 2023 Wolters Kluwer Health, Inc. All rights reserved.

Copyright © 2023 Wolters Kluwer Health, Inc. Unauthorized reproduction of this article is prohibited.

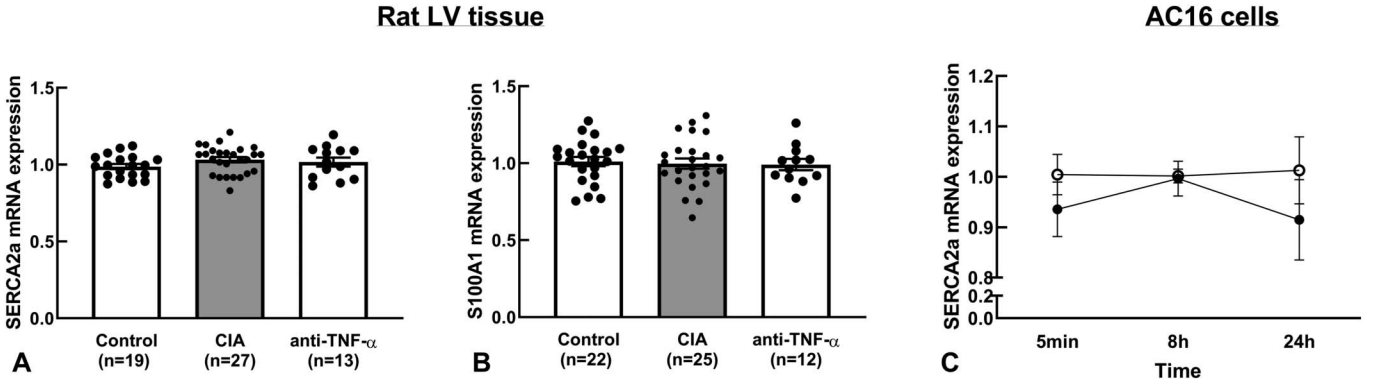


FIGURE 2. Expression of calcium handling genes in LV tissue and a cardiomyocyte cell line. Rats were inoculated with collagen (CIA) and subsequently treated with a TNF-α blocker (CIA+anti-TNF-α) before measurement of relative mRNA expression of *SERCA2a* (A) and *S100A1* (B) in LV tissue. mRNA expression of *SERCA2a* (C) was measured in AC16 cells without (open symbols) or with 10 ng/mL of TNF-α (filled symbols). Results are presented in arbitrary units normalized for the expression of the endogenous reference gene, *Hprt1* for LV tissue and *GAPDH* for AC16 cells, using the ΔΔCt method. Data are means ± SEM. For the AC16 cells, each data point represents the mean ± SEM for 3 independent experiments performed in quadruplicate.

which codes for the β-MyHC isoform, was increased in CIA rats (1.25 ± 0.05) compared with controls (0.96 ± 0.05, P = 0.0002). The relative mRNA expression of *Myh7* was significantly lower in the CIA+anti-TNF-α rats (0.91 ± 0.08) compared with CIA rats (1.25 ± 0.05, P = 0.0002, Fig. 6B). The *Myh6/Myh7* ratio of mRNA expression was decreased in CIA rats (0.79 ± 0.06) compared with controls (1.13 ± 0.07, P = 0.002), and compared with the CIA+anti-TNF-α rats (1.24 ± 0.09, P = 0.0004, Fig. 6C). These results suggest that increased circulating TNF-α, at least in part, mediates the inflammation-induced shifts in MyHC isoform gene expression in the CIA rats.

DISCUSSION

We have used the rat CIA model to study the preclinical pathogenesis of HFpEF induced by systemic inflammation. We have previously shown that collagen-induced systemic inflammation regulates many of the molecular mediators of passive diastolic processes.[18,19] We now show that systemic inflammation has no effect on the LV mRNA expression of the diastolic Ca^{2+}-regulating genes, *SERCA2a* and *S100A1*, the pro- and anti-apoptotic genes, *BAX* and *Bcl-2*, or the mitochondrial *SOD2* gene, which regulate active diastolic processes in LV tissue. Consistent with these in vivo results, TNF-α treatment had minimal effects on the expression of the *SERCA2a*, *S100A1*, *BAX*, and *Bcl-2* genes in the AC16 cardiomyocyte-derived cell line. Because we have shown that TNF-α does not mediate LV diastolic dysfunction, we assessed whether TNF-α may contribute to early-stage HFpEF pathogenesis by disrupting LV systolic function. Our STE results show impaired global longitudinal strain and global longitudinal velocity in the CIA rats, suggesting early-stage systolic dysfunction. These changes in systolic function were prevented by TNF-α blockade, indicating that TNF-α mediates the early-stage inflammation-induced LV systolic dysfunction. CIA rats exhibited decreased mRNA expression of *Myh6* (α-MyHC) and increased expression of *Myh7* (β-MyHC), which is associated with heart failure.[43] Blockade of TNF-α significantly increased the expression of *Myh6* and significantly decreased expression of *Myh7* in collagen-inoculated rats, indicating that TNF-α mediates the inflammation-induced changes in MyHC isotype expression. Taken together, our results suggest that increased circulating TNF-α stimulates a change in MyHC expression that affects contractile function and leads to early-stage systolic dysfunction. This, in turn, suggests that TNF-α contributes to early-stage pathogenesis of HFpEF by disrupting LV systolic, rather than diastolic, function.

It has been suggested that decreased expression of SERCA2a, which results in decreased Ca^{2+} uptake from the cytoplasm into the SR, contributes to the development of LV diastolic dysfunction[21,44] and it has been reported that LPS-induced severe acute inflammation decreased SERCA2a expression.[45] We found no change in the mRNA expression of *SERCA2a* or *S100A1* in CIA rats, suggesting that decreased SERCA2a expression is not the main contributor to inflammation-induced impaired myocardial diastolic relaxation. This is consistent with the work of Pironti et al[22] (2018) who showed no change in SERCA2a protein expression in mice with collagen antibody-induced arthritis, although cardiomyocytes from these mice showed impaired Ca^{2+} transients. The activity of the SERCA2a protein is regulated by phospholamban, which inhibits SERCA2a Ca^{2+} transport in its dephosphorylated state.[23] Thus, although we have shown no change in *SERCA2a* expression, there may be changes in the regulation of SERCA2a protein function that may alter Ca^{2+} transients independently of a change in its mRNA expression.

It is well known that TNF-α directly stimulates the extrinsic apoptosis pathway,[46] which is believed to cause cardiomyocyte loss and ultimately lead to impaired myocardial contractility in heart failure with reduced ejection fraction.[47] TNF-α exposure caused apoptosis in primary rat cardiomyocytes[48] and overexpression of TNF-α has been linked to a dilated heart associated

Copyright © 2023 Wolters Kluwer Health, Inc. All rights reserved.

Copyright © 2023 Wolters Kluwer Health, Inc. Unauthorized reproduction of this article is prohibited.

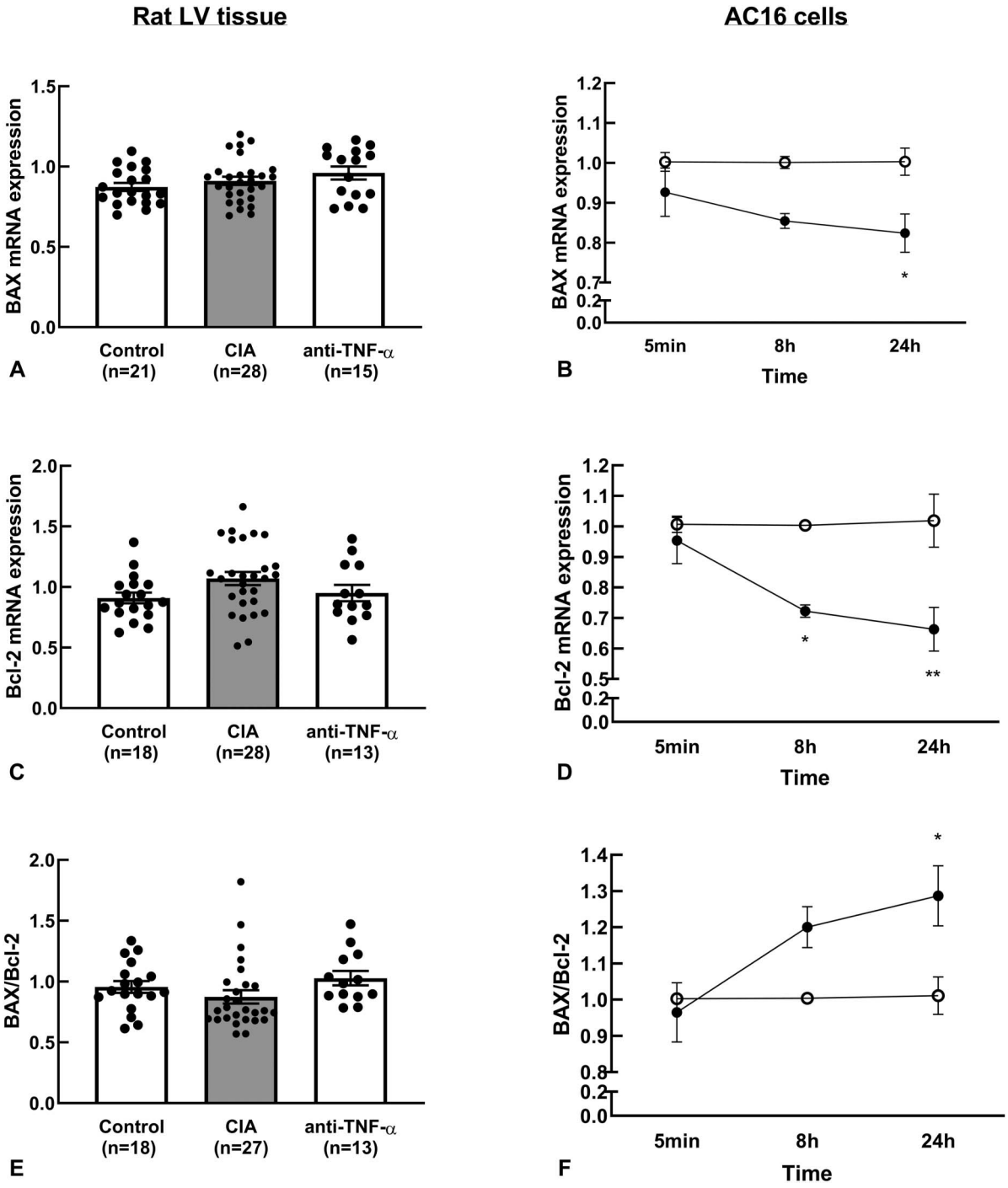


FIGURE 3. Expression of apoptotic genes in LV tissue and a cardiomyocyte cell line. Rats were inoculated with collagen (CIA) and subsequently treated with a TNF-α blocker (CIA+anti-TNF-α) before measurement of relative mRNA expression of *BAX* (A, B), *Bcl-2* (C, D) and the ratio of *BAX*/*Bcl-2* (E, F) in LV tissue (left panel) and in AC16 cells without (open symbols) or with 10 ng/mL of TNF-α (filled symbols) (right panel). Results are arbitrary units normalized for the expression of the endogenous reference gene, *Hprt1* for LV tissue and *GAPDH* for AC16 cells, using the ΔΔCt method. Data are means ± SEM. For the AC16 cells, each data point represents the mean ± SEM for 3 independent experiments performed in quadruplicate. $*P < 0.05$ versus control, $**P < 0.01$ versus control.

Copyright © 2023 Wolters Kluwer Health, Inc. All rights reserved.

Copyright © 2023 Wolters Kluwer Health, Inc. Unauthorized reproduction of this article is prohibited.

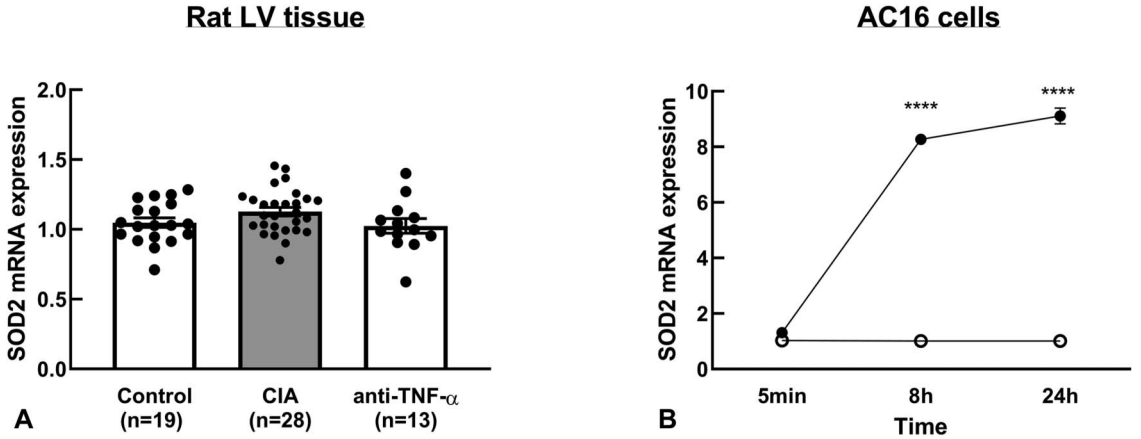


FIGURE 4. Expression of SOD2 in LV tissue and a cardiomyocyte cell line. Rats were inoculated with collagen (CIA) and subsequently treated with a TNF-α blocker (CIA+anti-TNF-α) before measurement of relative mRNA expression of *SOD2* in LV tissues (A) and in AC16 cells without (open symbols) or with 10 ng/mL of TNF-α (filled symbols) (B). Results are arbitrary units normalized for the expression of the endogenous reference gene, *Hprt1* for LV tissue and *GAPDH* for AC16 cells, using the ΔΔCt method. Data are means ± SEM. For the AC16 cells, each data point represents the mean ± SEM for 3 independent experiments performed in quadruplicate. ****$P < 0.0001$ versus control.

with systolic dysfunction with evidence of myocyte apoptosis in vivo.[49] It has also been suggested that increased mitochondrial reactive oxygen species (ROS) production[50,51] and cytoplasmic Ca^{2+} concentrations activate the intrinsic apoptosis pathway.[52,53] We showed no changes in LV mRNA expression of the pro-apoptotic *BAX* or the anti-apoptotic *Bcl-2* genes among any of the rat groups.

Although excess production of ROS stimulates apoptosis by disrupting mitochondrial integrity, physiological increases in ROS modulate many cellular signaling pathways, including expression of the ROS-neutralizing enzyme, SOD2, which prevents conversion of superoxide to highly reactive free radicals.[54] TNF-α also directly increases *SOD2* expression via activation of the NFκB transcription factor.[52,55] In the present study, the unchanged *SOD2* expression in the CIA rats suggests that the increased circulating TNF-α in the CIA rats may not be sufficient to activate *SOD2* expression in LV tissue. In contrast to the unchanged mRNA expression in CIA rats, mice with collagen antibody-induced arthritis showed increased local expression of SOD2 protein in heart tissue, along with impaired LV fractional shortening, a marker of myocardial systolic function.[22] In the present study, TNF-α stimulated increased expression of *SOD2* in AC16 cells. Although it has been suggested that TNF-α also stimulates mitochondrial ROS production in cardiomyocytes,[56] it is likely that the TNF-α-stimulated *SOD2* expression protects against ROS-induced apoptosis, as shown by the minimal changes in *BAX* expression and *BAX*/*Bcl-2* ratio in AC16 cells. In summary, as we have shown no changes in LV mRNA expression of any genes that affect active processes of LV diastolic function, namely *SERCA2a*, *S100A1*, *SOD2*, *BAX*, and *Bcl-2*, we cannot draw any firm conclusions about the effects of increased systemic inflammation on the active process of LV diastolic function.

Although increased circulating TNF-α has been reported to contribute to development of HFpEF,[34,35] we have shown that increased circulating TNF-α does not mediate LV diastolic dysfunction in CIA rats.[18] In contrast, although the CIA rats showed preserved ejection faction and unchanged fractional shortening, they showed impaired global longitudinal strain and global longitudinal velocity, indicating early-stage impairment of systolic function, similar to the preclinical systolic dysfunction observed in HFpEF patients. The changes in myocardial deformation (global longitudinal strain) and motion (global longitudinal velocity) were prevented by TNF-α blockade in the CIA+anti-TNF-α rats. These results show that increased systemic inflammation, and in particular increased circulating TNF-α, impair global longitudinal strain and global longitudinal velocity before the development of overt systolic dysfunction and reduced ejection fraction. This suggests that increased circulating TNF-α is an important contributor to inflammation-induced early-stage systolic dysfunction that may underlie development of HFpEF. We have previously shown that increased circulating TNF-α increases LV expression of profibrotic genes, LV fibrosis and extracellular matrix remodeling,[18] even though it does not mediate the LV diastolic dysfunction in CIA rats[18] (also see Table 1). The TNF-α dependence of fibrosis, but not LV diastolic dysfunction, implies that the fibrosis present in CIA rats does not contribute to the LV diastolic dysfunction that is present in the CIA rats and the CIA+anti-TNF-α rats (Table 1). Because it has been suggested that interstitial myocardial fibrosis may impair regional systolic function by decreasing heart wall motion and velocity,[57] the impaired systolic function in our CIA rats may arise, in part from TNF-α-mediated fibrosis.

Myocardial fibrosis has been associated with changes in expression patterns of MyHC isoforms.[58] The myosin motor molecule, a major component of the sarcomere, consists of 4 light chains and 2 heavy chains, of which there are 2 isoforms, α-MyHC encoded by the *Myh6* gene and β-MyHC encoded by *Myh7*.[58] The proportion of the heavy chain

Copyright © 2023 Wolters Kluwer Health, Inc. All rights reserved.

Copyright © 2023 Wolters Kluwer Health, Inc. Unauthorized reproduction of this article is prohibited.

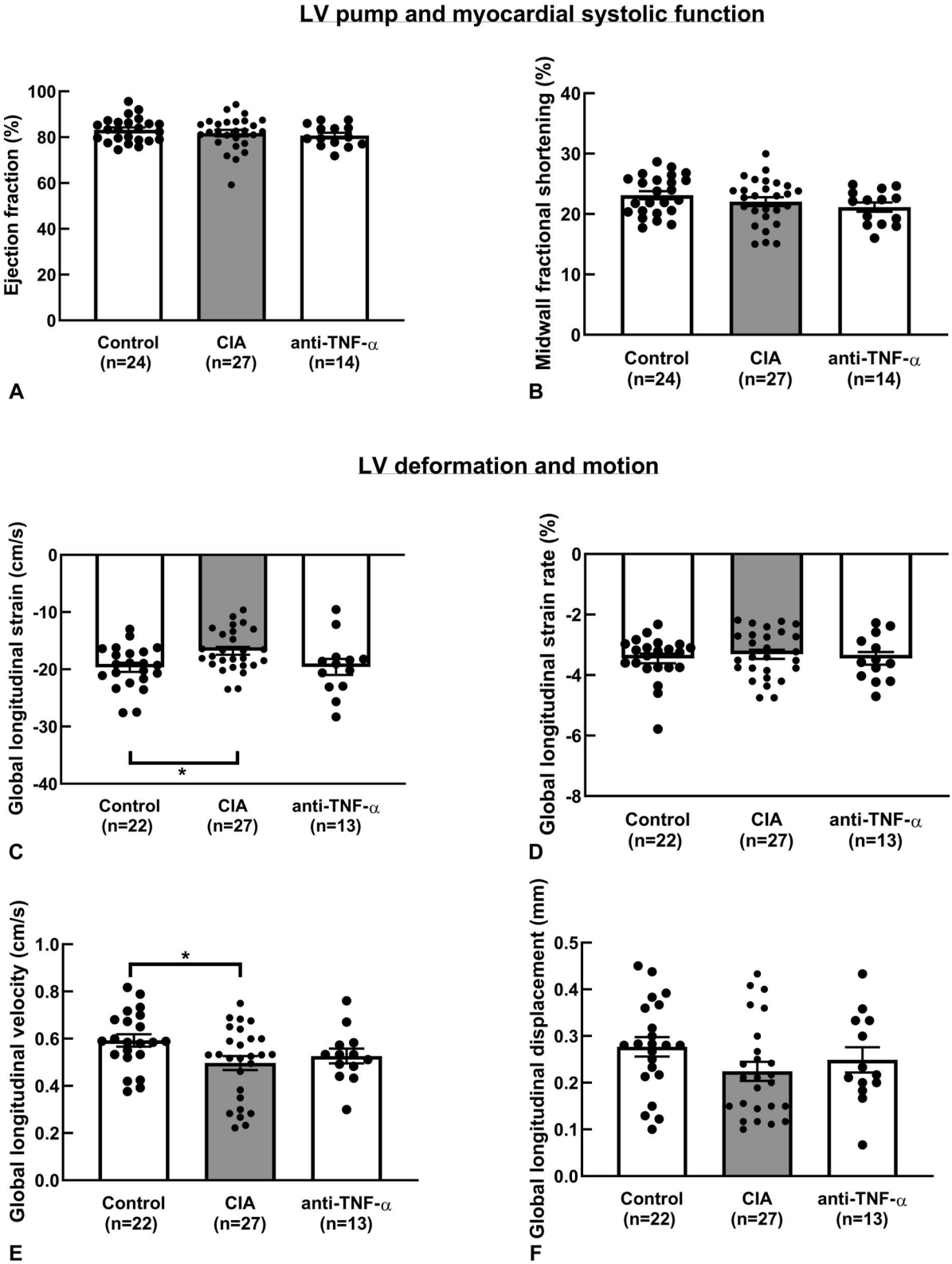


FIGURE 5. Echocardiographic measures of LV systolic function. Rats were inoculated with collagen to induce systemic inflammation (CIA) followed by treatment with a TNF-α blocker (CIA+anti-TNF-α) before STE measures of systolic function, ejection fraction (A), midwall fractional shortening (B), global longitudinal strain (C), global longitudinal strain rate (D), global longitudinal velocity (E), and global longitudinal displacement (F) were measured. Data are means ± SEM. *$P < 0.05$ versus control.

Copyright © 2023 Wolters Kluwer Health, Inc. All rights reserved.

Copyright © 2023 Wolters Kluwer Health, Inc. Unauthorized reproduction of this article is prohibited.

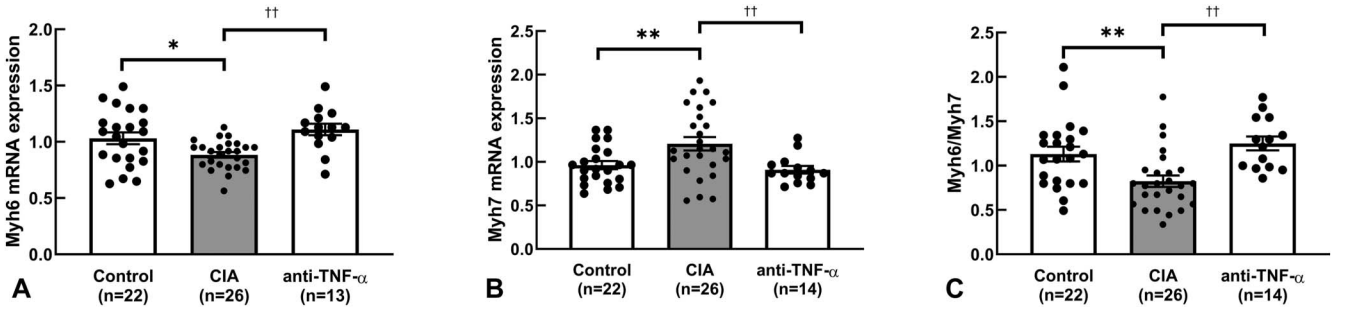


FIGURE 6. LV expression of contractility genes. Rats were inoculated with collagen (CIA) and treated with a TNF-α blocker (CIA+anti-TNF-α) before measurement of relative mRNA expression of *Myh6* (A), *Myh7* (B), and the ratio of *Myh6/Myh7* (C), in LV tissues. Relative mRNA expression results are arbitrary units normalized for the expression of the endogenous reference gene, *Hprt1*, using the ΔΔCt method. Data are from duplicate real time PCR experiments. Data presented as means ± SEM; $*P < 0.05$ versus control, $**P < 0.01$ versus control, $††P < 0.01$ versus CIA.

isoforms in LV tissues varies among species with small mammals having mostly α-MyHC, whereas healthy adult human LV has mostly β-MyHC with α-MyHC making up 7.2% of heavy chain protein and 33.3% of heavy chain mRNA expression.[59,60,62] The heavy chain isoform expression ratio varies in different regions of the LV wall and with physiological and pathophysiological conditions in humans and rodents.[58–64] It has been reported that the increased β-MyHC protein expression occurs primarily in myocytes located close to areas of fibrosis[58,61,65]**.** Failing human hearts have been shown to have severely decreased expression of the α-MyHC isoform,[59,60,62] decreasing the α-MyHC/β-MyHC ratio. In patients with heart failure, β-blocker treatment was shown to increase α-MyHC mRNA expression and decrease β-MyHC expression, resulting in an increased α-MyHC/β-MyHC ratio that correlated with improved systolic function.[66,67] Hypothyroidism, advancing age, pressure overload, and immune system activation increase β-MyHC expression in rodent models, decreasing the α-MyHC/β-MyHC ratio, whereas exercise and κ-opioid receptor agonist treatment have the opposite effect.[58,62,63,68] Inflammatory cytokines have also been shown to alter the ratio of α-MyHC to β-MyHC expression.[22,23] We have shown that CIA rats had decreased LV expression of *Myh6* and increased expression of *Myh7*, suggesting that early changes in MyHC isoform expression may precede the changes in contractile function that ultimately lead to systolic dysfunction and heart failure. We showed that blocking circulating TNF-α prevented the inflammation-induced shift in MyHC isoform expression observed in CIA rats. This shows that TNF-α is the major cytokine that mediates the inflammation-induced change in MyHC isoform expression. The changes in MyHC isoform expression are consistent with the changes in global longitudinal strain and velocity that are induced by inflammation and inhibited by blockade of circulating TNF-α. Therefore, the TNF-α-dependent changes in the MyHC isoform may underlie the TNF-α-dependent myocardial deformation and impaired motion.

LIMITATIONS

The main limitation of this study is the measurement of mRNA expression, which may not always correlate with protein expression and function, such as regulation of Ca^{2+} transients and the production and clearance of ROS, which must be investigated in future studies. The AC16 cells are dedifferentiated and therefore changes in gene expression may not fully mirror changes that happen in fully differentiated mature cardiomyocytes.[39,40] Because the effect of anti-TNF-α treatment was not evaluated in saline-treated rats, some of the effects reported may result from effects on baseline TNF-α in addition to counteracting the effects of CIA. The smaller sample size of the CIA+anti-TNF-α group reduces statistical power when comparisons are made with this group.

CONCLUSION

In conclusion, we have shown that systemic inflammation and TNF-α blockade have minimal effects on the expression of genes that are important in the active relaxation component of LV diastolic function. Although we cannot confirm that active processes of LV relaxation are not affected, our results are consistent with a previous suggestion that impaired Ca^{2+} sequestration and cardiomyocyte loss are more characteristic of heart failure with a reduced ejection fraction than of HFpEF.[46,69] In contrast, we have shown that collagen-induced systemic inflammation impaired early-stage LV systolic function and the ratio of α-MyHC/β-MyHC isoform expression, suggesting that disruption of MyHC isoform expression alters myocardial structure and function, which results in impaired systolic function. The prevention of the inflammation-induced alteration of MyHC isoform expression and LV systolic dysfunction by blockade of circulating TNF-α shows that increased circulating TNF-α may be a primary mediator of early-stage inflammation-induced LV systolic dysfunction. Hence, the contribution of increased circulating TNF-α to the early-stage pathogenesis of HFpEF is most likely via initiation of changes in cardiac muscle contractile properties that are characteristic of early-stage systolic dysfunction.

REFERENCES

1. Davis JM, Lin G, Oh JK, et al. Five-year changes in cardiac structure and function in patients with rheumatoid arthritis compared with the general population. *Int J Cardiol.* 2017;240:379–385.

Copyright © 2023 Wolters Kluwer Health, Inc. All rights reserved.

Copyright © 2023 Wolters Kluwer Health, Inc. Unauthorized reproduction of this article is prohibited.

2. Kobayashi M, Ferreira MB, Costa RQ, et al. Circulating biomarkers and cardiac structure and function in rheumatoid arthritis. *Front Cardiovasc Med.* 2021;8:754784.
3. Paulus WJ, Tschöpe C. A novel paradigm for heart failure with preserved ejection fraction: comorbidities drive myocardial dysfunction and remodeling through coronary microvascular endothelial inflammation. *J Am Coll Cardiol.* 2013;62:263–271.
4. Lewinter MM, Meyer M. Mechanisms of diastolic dysfunction in heart failure with a preserved ejection fraction. *Circ Heart Fail.* 2013;6:1112–1115.
5. Lewis GA, Schelbert EB, Williams SG, et al. Biological phenotypes of heart failure with preserved ejection fraction. *J Am Coll Cardiol.* 2017;70:2186–2200.
6. Lund LH, Savarese G. Global public health burden of heart failure. *Card Fail Rev.* 2017;03:7–11.
7. Nagueh SF. Heart failure with preserved ejection fraction: insights into diagnosis and pathophysiology. *Cardiovasc Res.* 2021;117:999–1014.
8. Wan SH, Vogel MW, Chen HH. Pre-clinical diastolic dysfunction. *J Am Coll Cardiol.* 2014;63:407–416.
9. Brucks S, Little WC, Chao T, et al. Contribution of left ventricular diastolic dysfunction to heart failure regardless of ejection fraction. *Am J Cardiol.* 2005;95:603–606.
10. Fukuta H, Little WC. Contribution of systolic and diastolic abnormalities to heart failure with a normal and a reduced ejection fraction. *Prog Cardiovasc Dis.* 2007;49:229–240.
11. Jasemian Y, Svendsen P, Deleuran B, Dagnaes-Hansen F. Refinement of the collagen induced arthritis model in rats by infrared thermography. *Br J Med Med Res.* 2011;1:469–477.
12. Yip G. Left ventricular long axis function in diastolic heart failure is reduced in both diastole and systole: time for a redefinition?. *Heart*. 2002;87:121–125.
13. Yu CM, Lin H, Yang H, et al. Progression of systolic abnormalities in patients with "isolated" diastolic heart failure and diastolic dysfunction. *Circulation*. 2002;105:1195–1201.
14. Le Roux R, Mokotedi L, Fourie S, et al. TNF-α inhibitors reduce inflammation-induced concentric remodelling, but not diastolic dysfunction in collagen-induced arthritis. *Clin Exp Rheumatol.* 2022;40:24–32.
15. Mokotedi L, Michel FS, Mogane C, et al. Associations of inflammatory markers with impaired left ventricular diastolic and systolic function in collagen-induced arthritis. *PLoS One*. 2020;15:e0230657.
16. Zile MR, Baicu CF, Ikonomidis JS, et al. Myocardial stiffness in patients with heart failure and a preserved ejection fraction. *Circulation*. 2015;131:1247–1259.
17. van Heerebeek L, Paulus W. Impact of comorbidities on myocardial remodeling and dysfunction in heart failure with preserved ejection fraction. *SOJ Pharm Sci.* 2014;1:20.
18. Manilall A, Mokotedi L, Gunter S, et al. Inflammation-induced left ventricular fibrosis is partially mediated by tumor necrosis factor-α. *Physiol Rep.* 2021;9:e15062.
19. Manilall A, Mokotedi L, Gunter S, et al. Increased protein phosphatase 5 expression in inflammation-induced left ventricular dysfunction in rats. *BMC Cardiovasc Disord.* 2022;22:539.
20. Biesiadecki BJ, Davis JP, Ziolo MT, Janssen PML. Tri-modal regulation of cardiac muscle relaxation; intracellular calcium decline, thin filament deactivation, and cross-bridge cycling kinetics. *Biophys Rev.* 2014;6:273–289.
21. Adeniran I, MacIver DH, Hancox JC, Zhang H. Abnormal calcium homeostasis in heart failure with preserved ejection fraction is related to both reduced contractile function and incomplete relaxation: an electromechanically detailed biophysical modeling study. *Front Physiol.* 2015;6:78.
22. Pironti G, Bersellini-Farinotti A, Agalave NM, et al. Cardiomyopathy, oxidative stress and impaired contractility in a rheumatoid arthritis mouse model. *Heart.* 2018;104:2026–2034.
23. Combes A, Frye C, Lemster B, et al. Chronic exposure to interleukin 1β induces a delayed and reversible alteration in excitation-contraction coupling of cultured cardiomyocytes. *Pflugers Archiv Eur J Physiol.* 2002;445:246–256.
24. McTiernan CF, Lemster BH, Frye C, et al. Interleukin-1 beta inhibits phospholamban gene expression in cultured cardiomyocytes. *Circ Res.* 1997;81:493–503.
25. Dunlay SM, Weston SA, Redfield MM, et al. Tumor necrosis factor-α and mortality in heart failure: a community study. *Circulation*. 2008;118:625–631.
26. Hanna A, Frangogiannis NG. Inflammatory cytokines and chemokines as therapeutic targets in heart failure. *Cardiovasc Drugs Ther.* 2020;34:849–863.
27. Baniaamam M, Handoko ML, Agca R, et al. The effect of anti-TNF therapy on cardiac function in rheumatoid arthritis: an observational study. *J Clin Med.* 2020;9:3145.
28. Sinagra E, Perricone G, Romano C, Cottone M. Heart failure and anti-tumor necrosis factor-alpha in systemic chronic inflammatory diseases. *Eur J Intern Med.* 2013;24:385–392.
29. Di Minno MND, Forte F, Tufano A, et al. Speckle tracking echocardiography in patients with systemic lupus erythematosus: a meta-analysis. *Eur J Intern Med.* 2020;73:16–22.
30. Hamdy AM. Use of strain and tissue velocity imaging for early detection of regional myocardial dysfunction in patients with beta thalassemia. *Eur J Echocardiography*. 2007;8:102–109.
31. Lo Gullo A, Rodríguez-Carrio J, Aragona CO, et al. Subclinical impairment of myocardial and endothelial functionality in very early psoriatic and rheumatoid arthritis patients: association with vitamin D and inflammation. *Atherosclerosis*. 2018;271:214–222.
32. Midtbø H, Semb AG, Matre K, et al. Disease activity is associated with reduced left ventricular systolic myocardial function in patients with rheumatoid arthritis. *Ann Rheum Dis.* 2017;76:371–376.
33. Sitia S, Tomasoni L, Atzeni F, et al. From endothelial dysfunction to atherosclerosis. *Autoimmun Rev.* 2010;9:830–834.
34. Ren M, Li X, Hao L, Zhong J. Role of tumor necrosis factor alpha in the pathogenesis of atrial fibrillation: a novel potential therapeutic target?. *Ann Med.* 2015;47:316–324.
35. Rolski F, Błyszczuk P. Complexity of TNF-α signaling in heart disease. *J Clin Med.* 2020;9:3267.
36. Billiau A, Matthys P. Modes of action of Freund's adjuvants in experimental models of autoimmune diseases. *J Leukoc Biol.* 2001;70:849–860.
37. Winter CA, Risley EA, Nuss GW. Carrageenin-induced edema in hind paw of the rat as an assay for antiinflammatory drugs. *Exp Biol Med.* 1962;111:544–547.
38. Sharifov OF, Schiros CG, Aban I, et al. Diagnostic accuracy of tissue Doppler index E/e' for evaluating left ventricular filling pressure and diastolic dysfunction/heart failure with preserved ejection fraction: a systematic review and meta-analysis. *J Am Heart Assoc.* 2016;5:e002530.
39. Davidson M, Nesti C, Palenzuela L, et al. Novel cell lines derived from adult human ventricular cardiomyocytes. *J Mol Cell Cardiol.* 2005;39:133–147.
40. Onódi Z, Visnovitz T, Kiss B, et al. Systematic transcriptomic and phenotypic characterization of human and murine cardiac myocyte cell lines and primary cardiomyocytes reveals serious limitations and low resemblances to adult cardiac phenotype. *J Mol Cell Cardiol.* 2022;165:19–30.
41. Livak KJ, Schmittgen TD. Analysis of relative gene expression data using real-time quantitative PCR and the $2^{-\Delta\Delta CT}$ method. *Methods*. 2001;25:402–408.
42. *RefFinder Algorithm Software (RefFinderWebsite)*. Available at: http://blooge.cn/RefFinder/
43. Vigil-Garcia M, Demkes CJ, Eding JEC, et al. Gene expression profiling of hypertrophic cardiomyocytes identifies new players in pathological remodelling. *Cardiovasc Res.* 2020;117:1532–1545.
44. Park J-H, Marwick TH. Use and limitations of E/e' to assess left ventricular filling pressure by echocardiography. *J Cardiovasc Ultrasound*. 2011;19:169.
45. Tsai CT, Wu CK, Lee JK, et al. TNF- down-regulates sarcoplasmic reticulum Ca2+ ATPase expression and leads to left ventricular diastolic dysfunction through binding of NF- B to promoter response element. *Cardiovasc Res.* 2015;105:318–329.
46. Keystone EC, Ware CF. Tumor necrosis factor and anti-tumor necrosis factor therapies. *J Rheumatol Suppl.* 2010;85:27–39.
47. Simmonds SJ, Cuijpers I, Heymans S, Jones EAV. Cellular and molecular differences between HFpEF and HFrEF: a step ahead in an improved pathological understanding. *Cells*. 2020;9:242.
48. Krown KA, Page MT, Nguyen C, et al. Tumor necrosis factor alpha-induced apoptosis in cardiac myocytes. Involvement of the sphingolipid

Copyright © 2023 Wolters Kluwer Health, Inc. All rights reserved.

Copyright © 2023 Wolters Kluwer Health, Inc. Unauthorized reproduction of this article is prohibited.

signaling cascade in cardiac cell death. *J Clin Invest.* 1996;98:2854–2865.
49. Bryant D, Becker L, Richardson J, et al. Cardiac failure in transgenic mice with myocardial expression of tumor necrosis factor-α. *Circulation*. 1998;97:1375–1381.
50. Dubois-Deruy E, Peugnet V, Turkieh A, Pinet F. Oxidative stress in cardiovascular diseases. *Antioxidants*. 2020;9:864.
51. Peoples JN, Saraf A, Ghazal N, et al. Mitochondrial dysfunction and oxidative stress in heart disease. *Exp Mol Med.* 2019;51:1–13.
52. Hajnóczky G, Davies E, Madesh M. Calcium signaling and apoptosis. *Biochem Biophysical Res Commun.* 2003;304:445–454.
53. Orrenius S, Zhivotovsky B, Nicotera P. Regulation of cell death: the calcium–apoptosis link. *Nat Rev Mol Cell Biol.* 2003;4:552–565.
54. Miao L, St Clair DK. Regulation of superoxide dismutase genes: implications in disease. *Free Radic Biol Med.* 2009;47:344–356.
55. Marelli-Berg FM, Aksentijevic D. Immunometabolic cross-talk in the inflamed heart. *Cell Stress*. 2019;3:240–266.
56. Roberge S, Roussel J, Andersson DC, et al. TNF-mediated caspase-8 activation induces ROS production and TRPM2 activation in adult ventricular myocytes. *Cardiovasc Res.* 2014;103:90–99.
57. Maragiannis D, Alvarez PA, Ghosn MG, et al. Left ventricular function in patients with hypertrophic cardiomyopathy and its relation to myocardial fibrosis and exercise tolerance. *Int J Cardiovasc Imaging*. 2018;34:121–129.
58. Pandya K, Kim HS, Smithies O. Fibrosis, not cell size, delineates beta-myosin heavy chain reexpression during cardiac hypertrophy and normal aging in vivo. *Proc Natl Acad Sci.* 2006;103:16864–16869.
59. Miyata S, Minobe W, Bristow MR, Leinwand LA. Myosin heavy chain isoform expression in the failing and non-failing human heart. *Circ Res.* 2000;86:386–390.
60. Nakao K, Minobe W, Roden R, et al. Myosin heavy chain gene expression in human heart failure. *J Clin Invest.* 1997;100:2362–2370.
61. Pandya K, Smithies O. β-MyHC and cardiac hypertrophy. *Circ Res.* 2011;109:609–610.
62. Walklate J, Ferrantini C, Johnson CA, et al. Alpha and beta myosin isoforms and human atrial and ventricular contraction. *Cell. Mol. Life Sci.* 2021;78:7309–7337.
63. Fitzsimons DP, Patel JR, Moss RL. Role of myosin heavy chain composition in kinetics of force development and relaxation in rat myocardium. *J Physiol.* 1998;513:171–183.
64. Carniel E, Taylor MRG, Sinagra G, et al. α-Myosin heavy chain: a sarcomeric gene associated with dilated and hypertrophic phenotypes of cardiomyopathy. *Circulation*. 2005; 112: 54–59.
65. López JE, Myagmar BE, Swigart PM, et al. β-Myosin heavy chain is induced by pressure overload in a minor subpopulation of smaller mouse cardiac myocytes. *Circ Res.* 2011;109:629–638.
66. Lowes BD, Gilbert EM, Abraham WT, et al. Myocardial gene expression in dilated cardiomyopathy treated with beta-blocking agents. *N Engl J Med.* 2002;346:1357–1365.
67. Yasumura Y, Takemura K, Sakamoto A, et al. Changes in myocardial gene expression associated with β-blocker therapy in patients with chronic heart failure. *J Card Fail.* 2003;9:469–474.
68. Jaiswal A, Kumar S, Seth S, et al. Effect of U50,488H, a κ-opioid receptor agonist on myocardial α-and β-myosin heavy chain expression and oxidative stress associated with isoproterenol-induced cardiac hypertrophy in rat. *Mol Cell. Biochem.* 2010;345:231–240.
69. Peana D, Domeier TL. Cardiomyocyte Ca 2+ homeostasis as a therapeutic target in heart failure with reduced and preserved ejection fraction. *Curr Opin Pharmacol.* 2017;33:17–26.

Copyright © 2023 Wolters Kluwer Health, Inc. All rights reserved.

Copyright © 2023 Wolters Kluwer Health, Inc. Unauthorized reproduction of this article is prohibited.